

Supporting information:

Carboxyl-Alkyl Functionalized Conjugated Polyelectrolytes for High Performance Organic Electrochemical Transistors

Zeyuan Sun¹, Brian Khau^{2#}, Hao Dong¹, Christopher J Takacs³, Shuhan Yuan⁴, Mengting Sun¹, Bar Mosevitzky Lis¹, Dang Nguyen¹, Elsa Reichmanis^{1,*}

¹Department of Chemical and Biomolecular Engineering, Lehigh University, Bethlehem, PA, 18015, USA

²School of Chemical and Biomolecular Engineering, Georgia Institute of Technology, Atlanta, GA 30332, United States

³Stanford Synchrotron Radiation Lightsource SLAC National Accelerator Laboratory, Menlo Park, CA 94025, United States

⁴Department of Applied Health Science, School of Public Health, Indiana University, Bloomington, IN 47405, United States

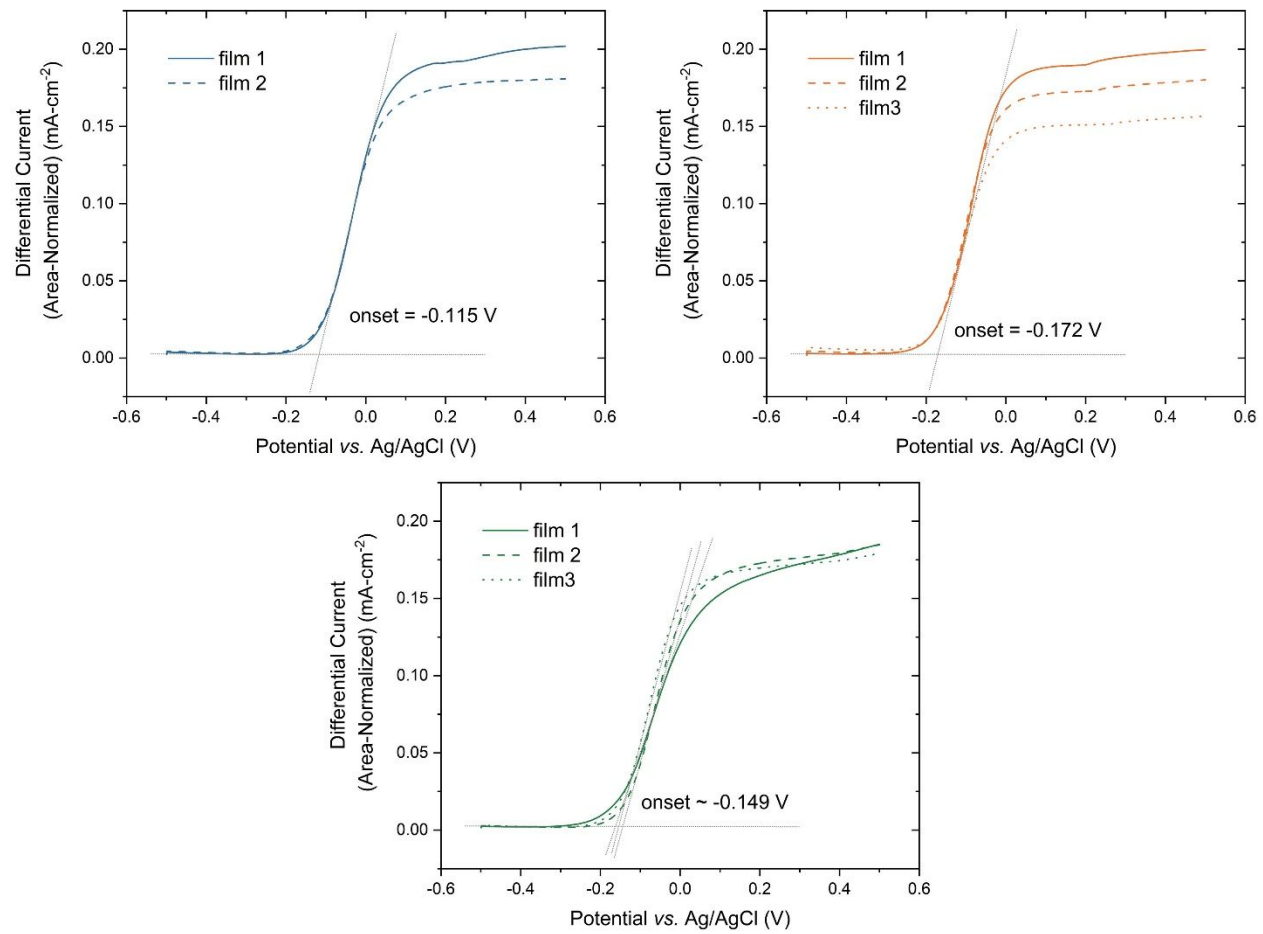


Figure S1: Differential Pulse Voltammetry (DPV) for P3C(Pr)T (blue), P3C(Bu)T (orange), and P3C(Pe)T (green), in 0.1 M NaCl in H₂O. The measured onset is vs. the Ag/AgCl reference.

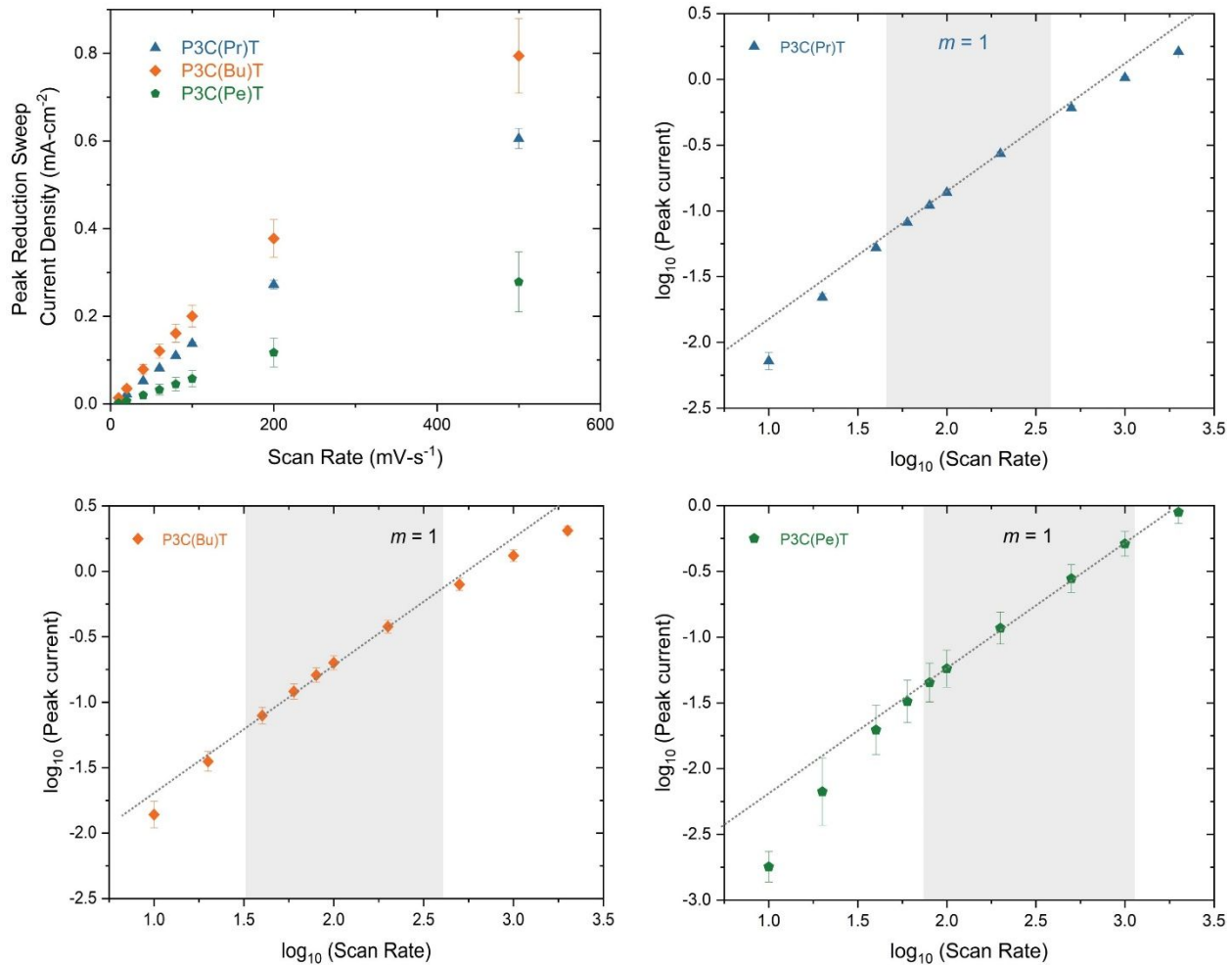


Figure S2: Top left: Linear graph of peak reduction current density as a function of scan rate. Top right; bottom left; bottom right: log-log plots for peak density vs scan rate for P3C(Pr)T (blue), P3C(Bu)T (orange), and P3C(Pe)T (green), in 0.1 M NaCl (aq) to analyze power scaling for mass transfer limitations.

Table S1: Approximate regimes cutoffs for the polymers tested in this study

Polymers	Superlinear (Diffusion-limited)	Linear (Adsorption-limited)	Square-Root (Mass transfer limited)
P3C(Pr)T	< 50 $\text{mV}\cdot\text{s}^{-1}$	50-500 $\text{mV}\cdot\text{s}^{-1}$	> 500 $\text{mV}\cdot\text{s}^{-1}$
P3C(Bu)T	< 50 $\text{mV}\cdot\text{s}^{-1}$	50-300 $\text{mV}\cdot\text{s}^{-1}$	> 300 $\text{mV}\cdot\text{s}^{-1}$
P3C(Pe)T	< 100 $\text{mV}\cdot\text{s}^{-1}$	100-1000 $\text{mV}\cdot\text{s}^{-1}$	> 1000 $\text{mV}\cdot\text{s}^{-1}$

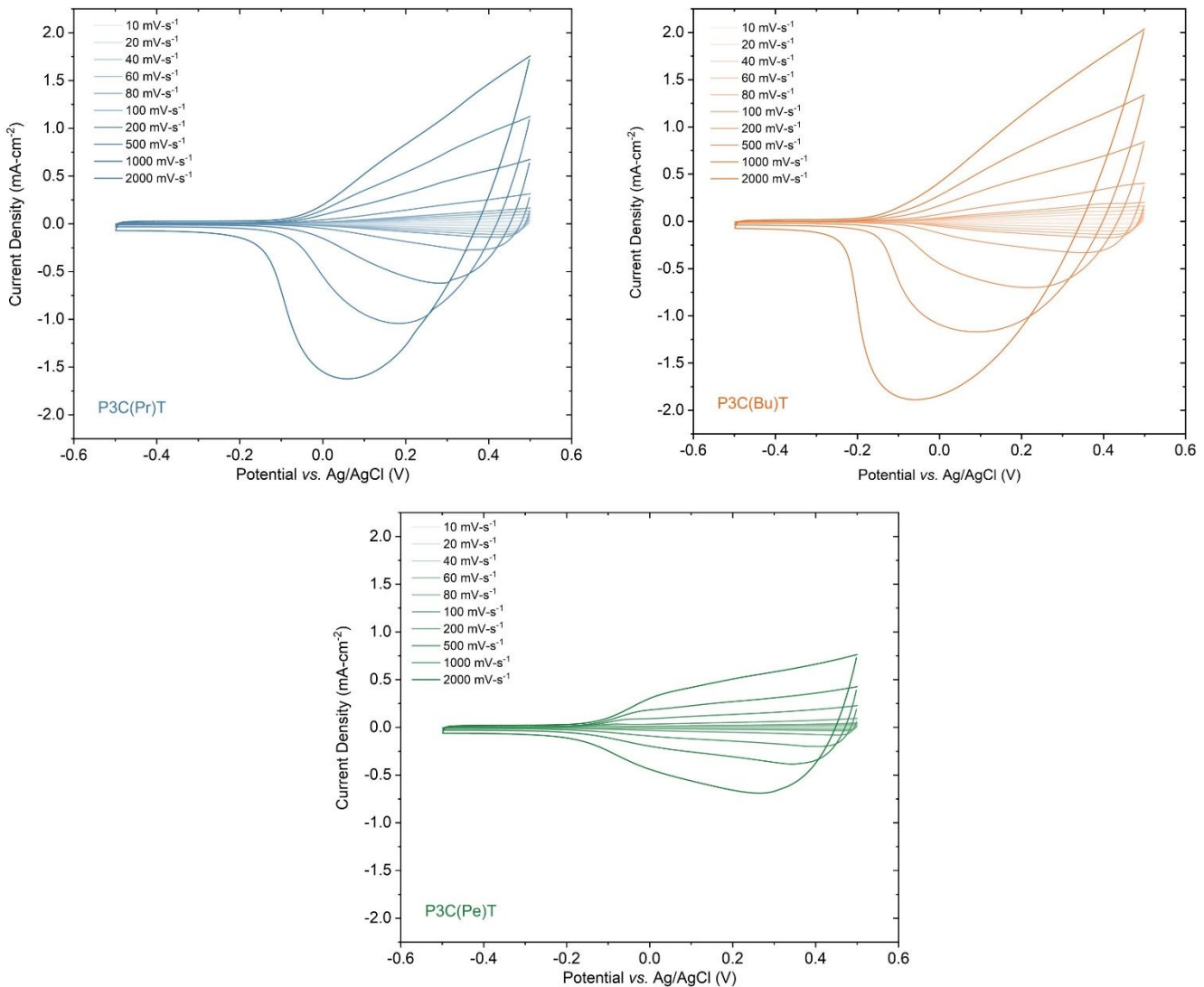


Figure S3: Cyclic Voltammograms of P3C(Pr)T (blue), P3C(Bu)T (orange), and P3C(Pe)T (green) taken at increasing scan rates from 10 – 2000 mV/s in 0.1 NaCl (aq).

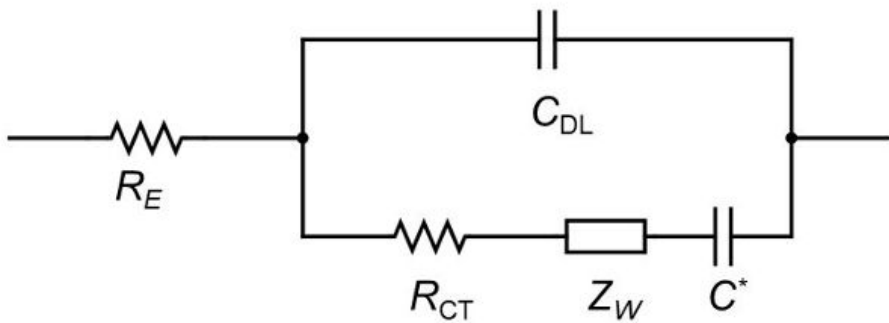


Figure S4: Schematic of the diffusion-modified Randles circuit

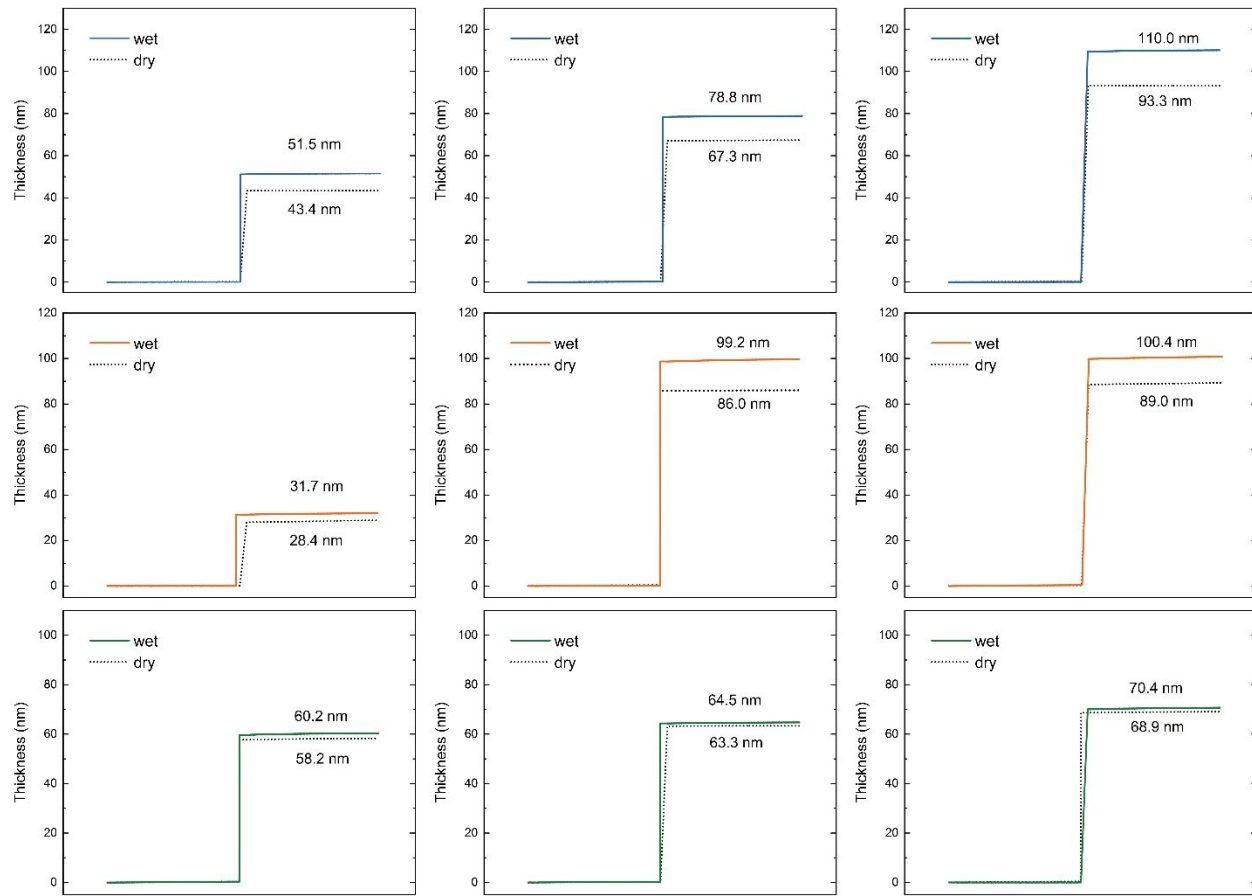


Figure S5. Sauerbrey-derived thickness from the 7th harmonic of the QCM-D for P3C(Pr)T (blue), P3C(Bu)T (orange), and P3C(Pe)T (green) in the wet and dry state.

Table S2: Dry and wet thicknesses as well as averaged swelling percentage calculated using the Sauerbrey equation for P3CATs thin film in 0.1 M NaCl solution.

Polymers	Dry Thickness [nm]	Wet Thickness [nm]	Average Swelling Percentage [%]
P3C(Pr)T	43.4 / 67.3 / 93.3	51.5 / 78.8 / 110.0	17.9
P3C(Bu)T	28.4 / 86.0 / 89.0	31.7 / 99.2 / 100.4	12.3
P3C(Pe)T	58.2 / 63.3 / 68.9	60.2 / 64.5 / 70.4	2.5

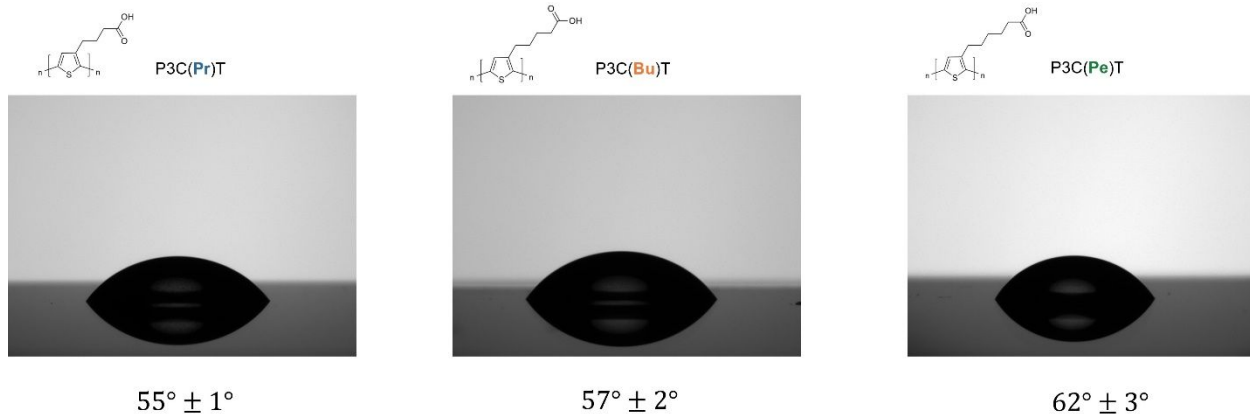


Figure S6. Water contact angle measurement of thin films for P3C(Pr)T (blue), P3C(Bu)T (orange), and P3C(Pe)T (green) average from five samples.

Table S3: Summary of passive swelling of organic mixed conductors in different solvents/electrolyte.

Polymers	Solvent/Electrolyte	Passive Swelling [%]
P3C(Pr)T (this work)	H ₂ O/NaCl	17.9%
P3C(Bu)T (this work)	H ₂ O/NaCl	12.3%
P3C(Pe)T (this work)	H ₂ O/NaCl	2.5%
P3HHT ¹	H ₂ O/KCl	2.4%
PEDOT:PSS ²	H ₂ O/NaCl	86%
p(g2T-TT) ³	H ₂ O/NaCl	10%
p(p2T-TT) ⁴	H ₂ O/NaCl	5%
p(b2T-TT) ⁴	H ₂ O/NaCl	13%
p(gNDI-gT2) ⁵	H ₂ O/NaCl	44%
p(C3-gNDI-gT2) ⁵	H ₂ O/NaCl	28%
p(C6-gNDI-gT2) ⁵	H ₂ O/NaCl	13%
PTHS-TMA+-co-P3HT 51:49 mol ⁶	H ₂ O/NaCl	22%
PTHS-TMA+-co-P3HT 23:77 mol ⁶	H ₂ O/NaCl	4%
p(g3T2) ⁷	H ₂ O/NaCl	50%

If not otherwise specified, swelling measurement was conducted through QCM-D. **P3HHT** is a polythiophenes with hexyl-hydroxyl side chain. **PEDOT:PSS** is poly(3,4-ethylenedioxythiophene):polystyrene sulfonate. **p(g2T-TT)** is poly(2-(3,3-bis(2-(2-methoxyethoxy) ethoxy)-[2,20-bithiophen]-5-yl)thieno[3,2-b]thiophene). **p(p2T-TT)** and **p(b2T-TT)** are the derivatives by replacing the ethylene glycol side chain on p(g2T-TT) with propylene glycol (PG) and butylene glycol (BG), respectively. **p(gNDI-gT2)** is a copolymer comprising glycolated naphthalene-tetracarboxylic diimide-bithiophene (gNDI-T2) units bearing with ethylene glycol side chain, and **p(C3-gNDI-gT2)** and **p(C6-gNDI-gT2)** are derivatives featuring either a propyl or a hexyl glycol chains on NDI-T2 backbone. **PTHS** is a polythiophene with hexanesulfonate side chain, **PTHS-TMA+** is PTHS that has a cation-exchanged tetramethylammonium group. **PTHS-TMA+-co-P3HT** is a gradient copolymer consisting of PTHS and poly(3-hexylthiophene) (P3HT). **p(g3T2)** is poly[3,3'-bis(2-(2-(2-methoxyethoxy)ethoxy)-2,2'-bithiophene].

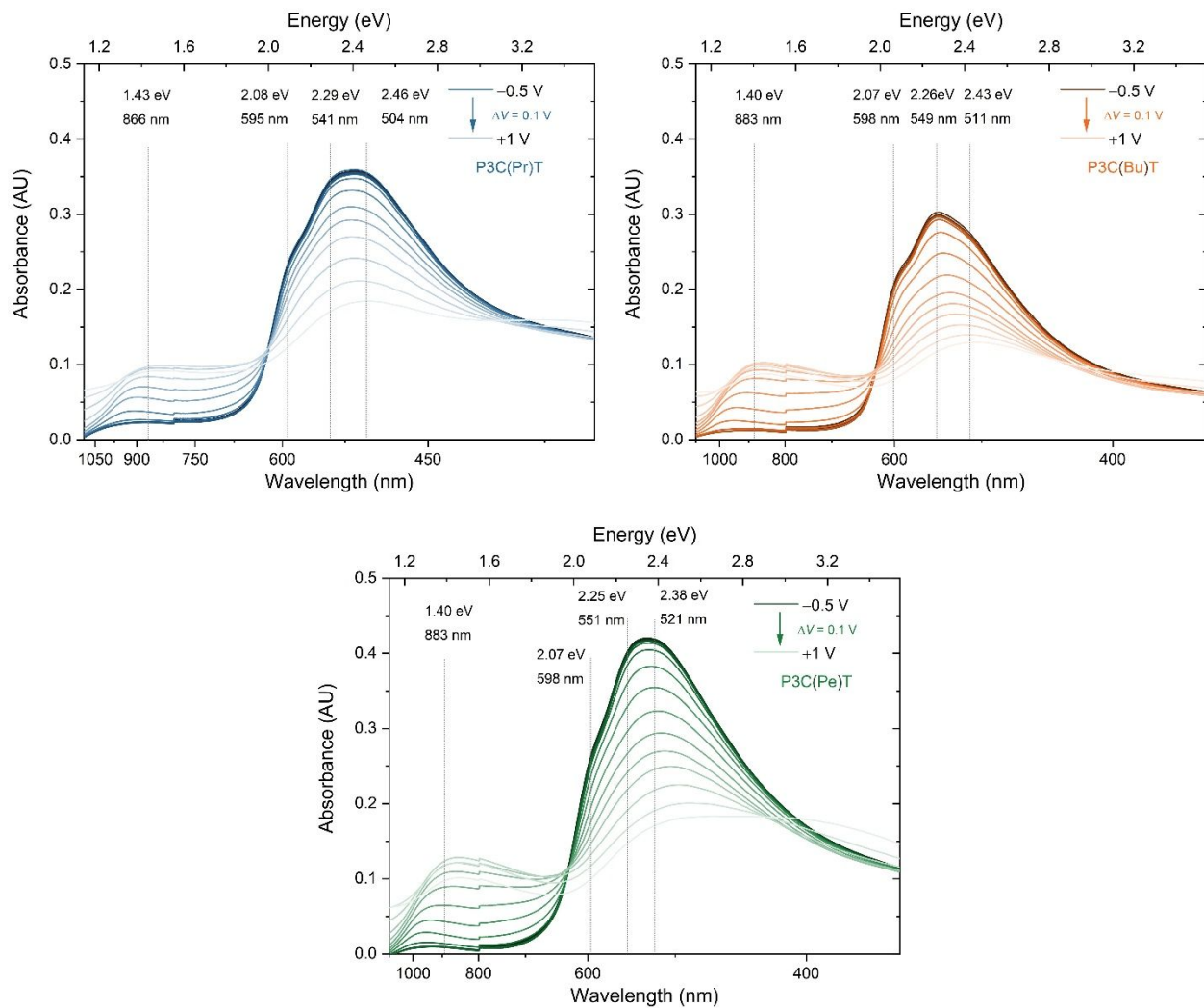


Figure S7: Non-normalized voltage-dependent UV-Vis-NIR steady state spectra of P3C(Pr)T (blue), P3C(Bu)T (orange), and P3C(Pe)T (green) from -0.5 V (dark) to 1 V (light) vs. Ag/AgCl in 0.1 M NaCl (*aq*) in 0.1 V increments of as-cast film on ITO/glass.

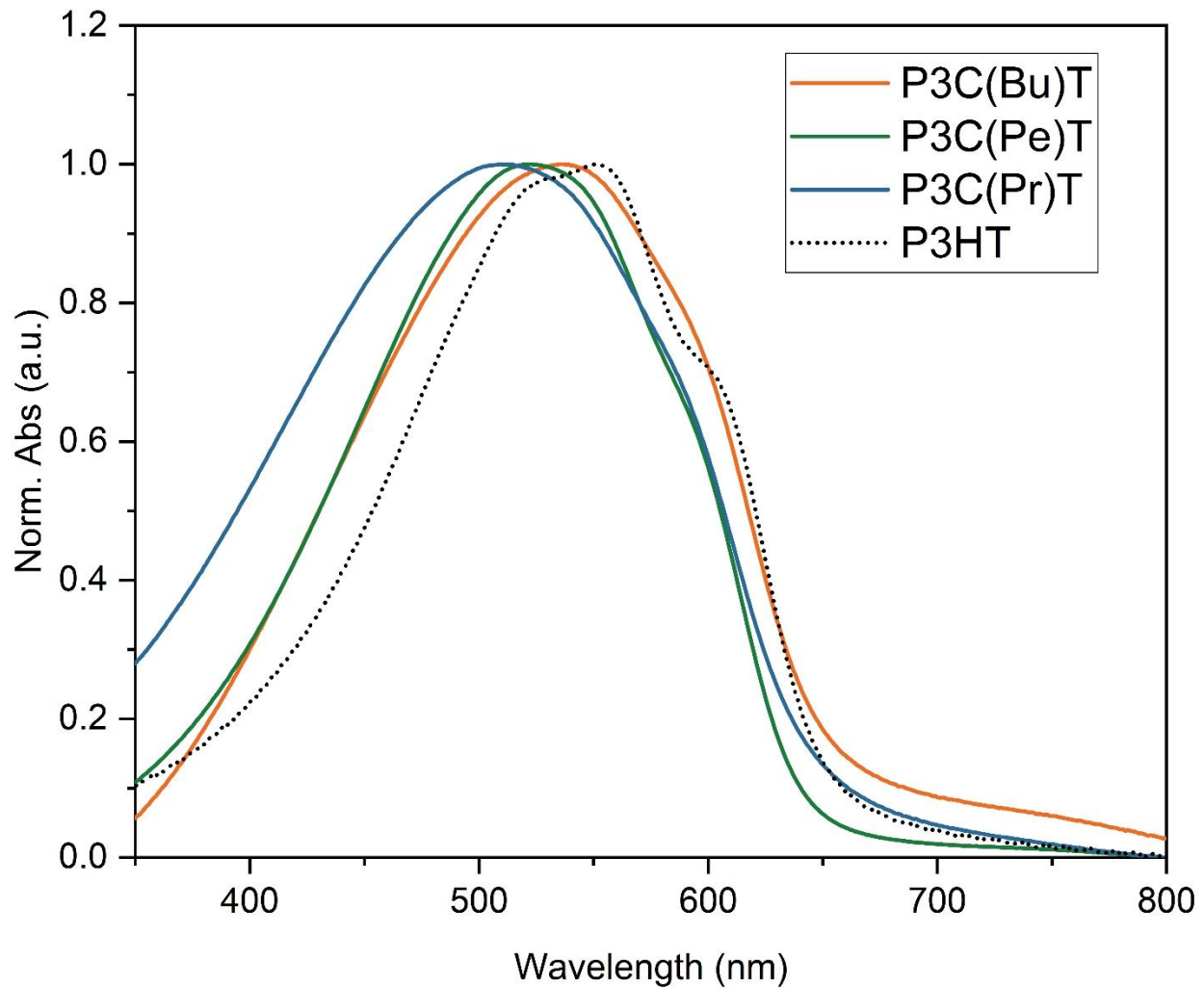


Figure S8: Comparison of steady-state UV-Vis of pristine films in ambient condition for P3HT (dot), P3C(Pr)T (blue), P3C(Bu)T (orange), and P3C(Pe)T (green)

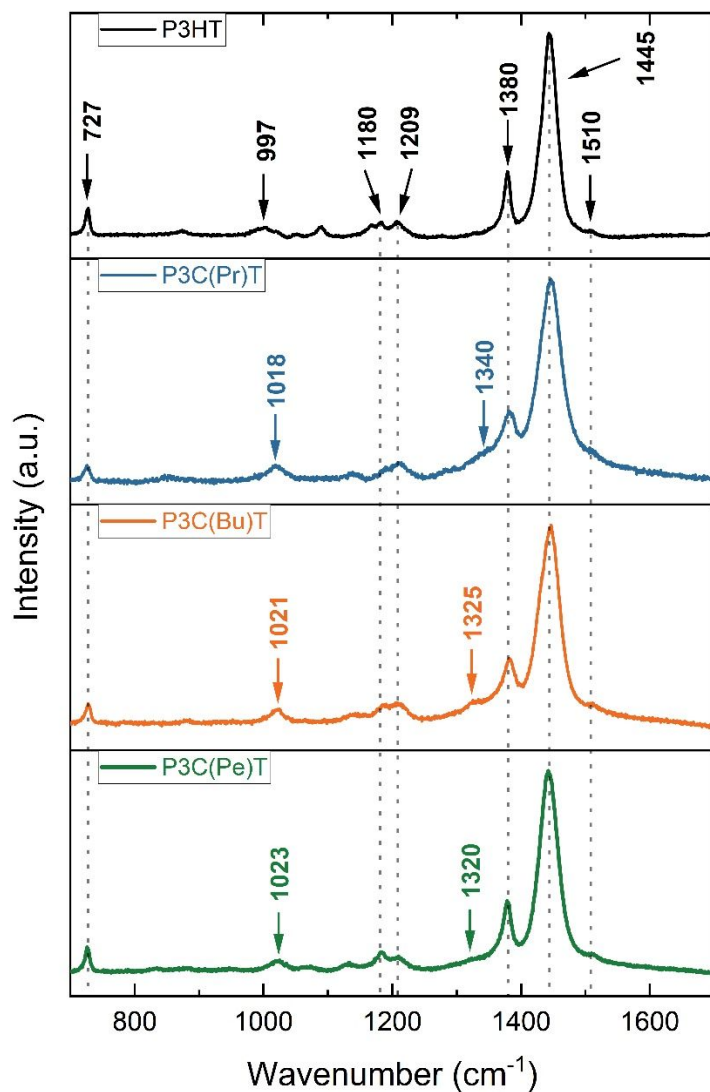


Figure S9: *ex situ* Raman spectra under 633 nm excitation wavelength for P3HT (black), P3C(Pr)T (blue), P3C(Bu)T (orange), and P3C(Pe)T (green) in air.

Table S4: Summary of P3HT and P3CATs Raman Peak assignment under 633 nm.

Mode #	P3HT Peak position (cm ⁻¹)	P3CATs Peak position (cm ⁻¹)	P3HT Literatures positions (cm ⁻¹) ⁸	Mode Assignment
1	1510	1510	1512	Antisymmetric C=C stretching
2	1445	1445	1443	Symmetric C=C stretching
3	1380	1380	1378	Intra-ring C-C stretching
4	1209	1209	1208	Inter-ring C-C stretching
5	1180	1180	1186	C-H bending with Inter-ring C-C stretching
6	997	1018/1021/1023	1021	C-C alkyl stretching
7	727	727	728	C-S-C deformation

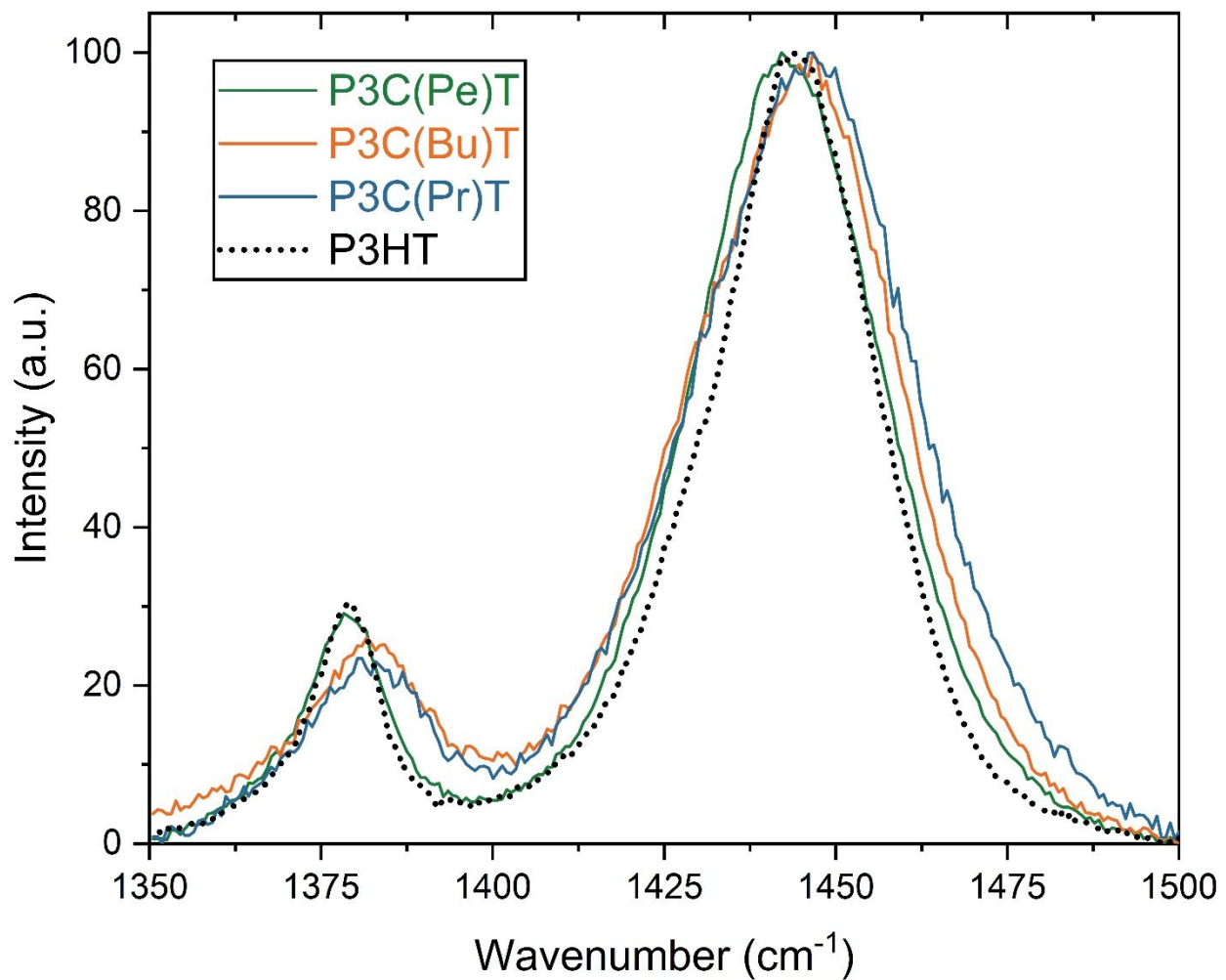


Figure S10: Comparison of *ex situ* Raman spectra of pristine films under 633 nm excitation wavelength between 1350 to 1500 cm⁻¹ in ambient condition for P3HT (dot), P3C(Pr)T (blue), P3C(Bu)T (orange), and P3C(Pe)T (green).

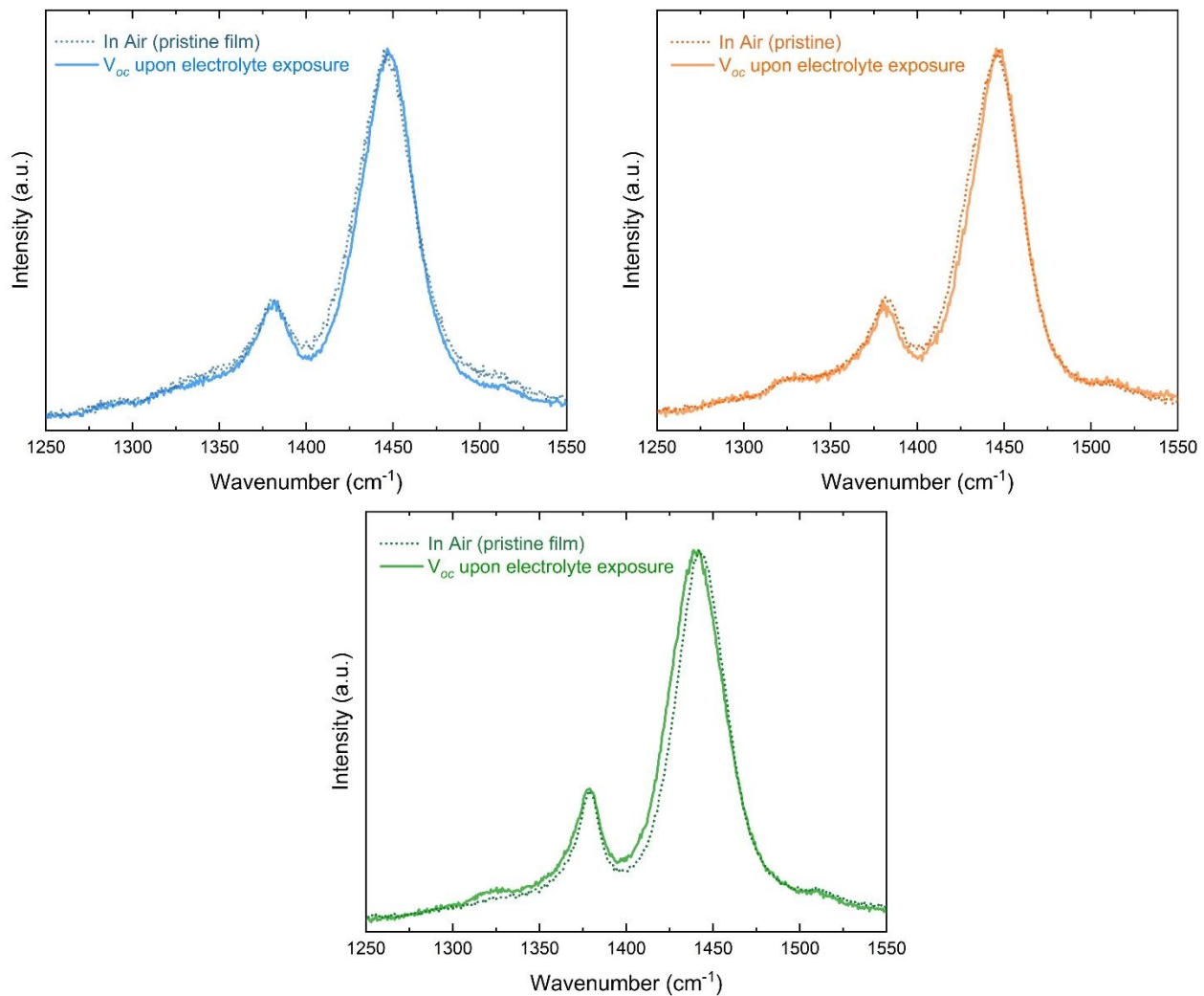


Figure S11: *ex situ* Raman spectra for each polymer, P3C(Pr)T (blue), P3C(Bu)T (orange), and P3C(Pe)T (green) in air condition compared with immediately exposing to electrolyte.

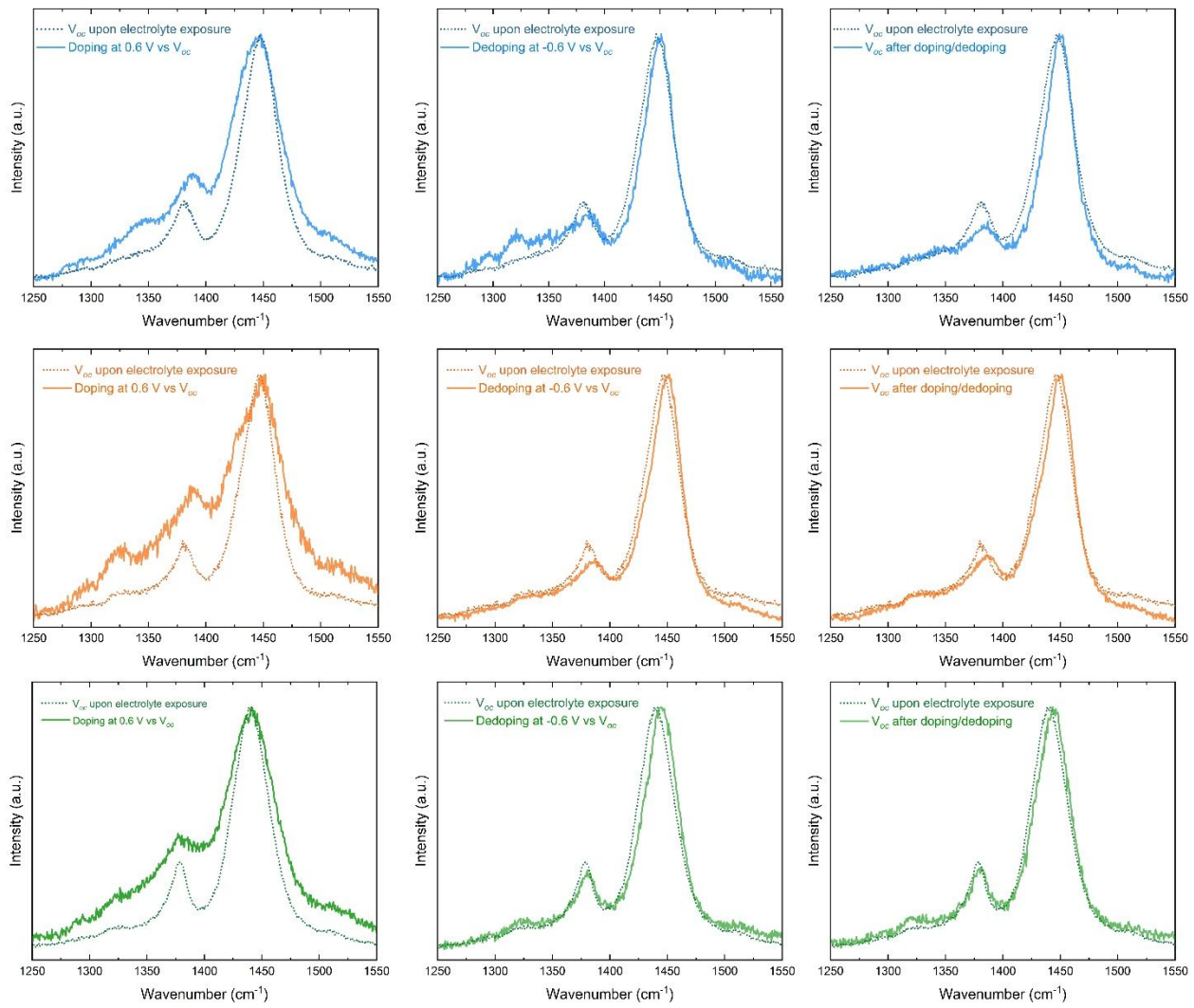


Figure S12: *in situ* Raman spectra comparison with initial V_{oc} for each polymer at doping, dedoping and V_{oc} state after doping/dedoping cycles.

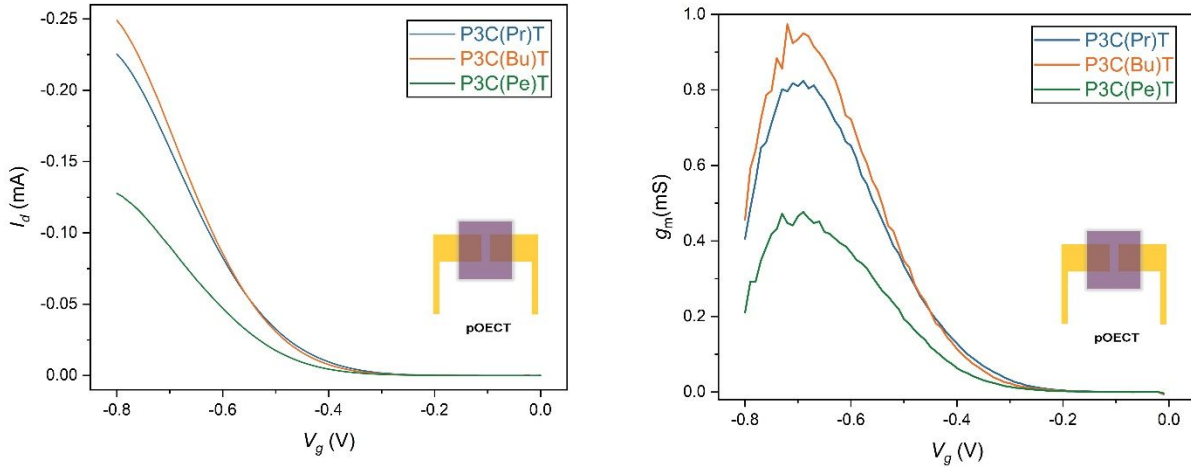


Figure S13. Example of pOECT characteristics ($W = 100 \mu\text{m}$, $L = 50 \mu\text{m}$) for P3C(Pr)T (138 nm, blue), P3C(Bu)T (100 nm, orange), and P3C(Pe)T (140 nm, green). From left to right, Transfer curve ($V_d = -0.6$ V) showing drain current varied with gate and transconductance curve.

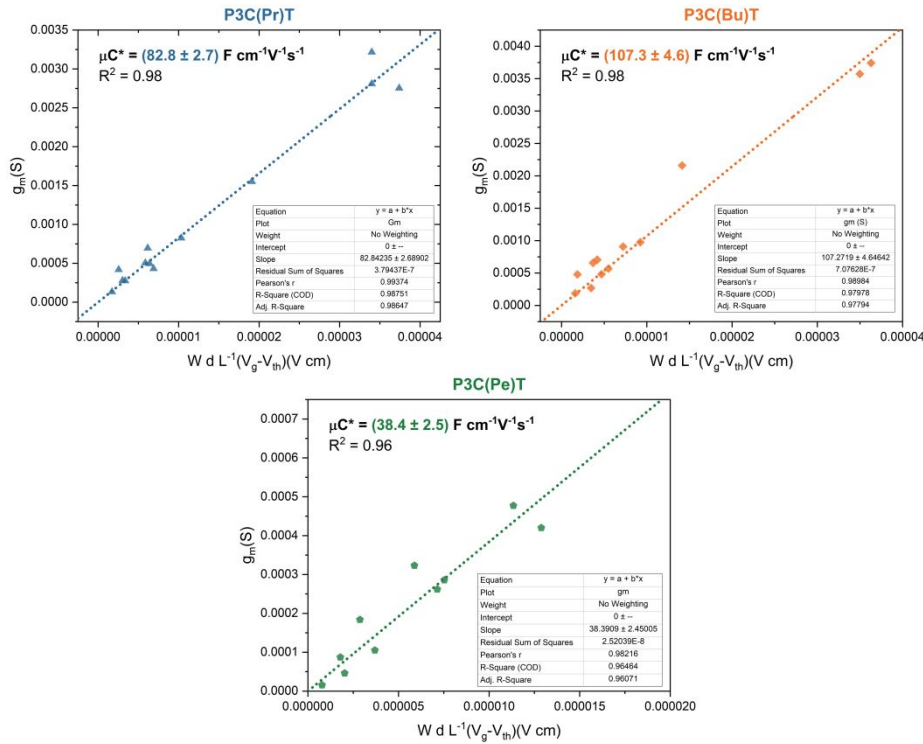


Figure S14: Transconductance values as a function of channel geometry in a linear scale for P3C(Pr)T (blue), P3C(Bu)T (orange), and P3C(Pe)T (green) from left to right. Dashed lines are the linear fits $y = ax$, and μC^* values are extracted from the slope of the linear fit.

Table S5: Summary of figure-of-merit parameters for conjugated polyelectrolytes. For interdigitated iOECT comparison, all interdigitated electrodes used in this work have a channel length $L = 10$ um, and total width: $W = 90$ (finger number) $\times 2.75$ mm (finger width) = 247.5 mm

Polymers	Electrolyte	μC^* [F cm $^{-1}$ V $^{-1}$ s $^{-1}$]	C^* [F cm $^{-3}$]	g_m, iOECT [mS]	d_{iOECT} [nm]	$[Wd/L]_{\text{iOECTs}}$ [mm]
P3C(Pr)T	0.1 M H ₂ O/NaCl	83 ± 3	145 ± 18	158	100	2.5
P3C(Bu)T	0.1 M H ₂ O/NaCl	107 ± 4	111 ± 14	159	89	2.2
P3C(Pe)T	0.1 M H ₂ O/NaCl	38 ± 3	30 ± 5	149	95	2.4
PTHS + EG ⁹	0.1 M H ₂ O/NaCl	5.5 ± 0.1	124	-	-	-
PTHS-TMA+-co-P3HT 70:30 mol ⁶	0.1 M H ₂ O/NaCl	0.97	107 ± 6	-	-	-
PTHS-TMA+-co-P3HT 51:49 mol ⁶	0.1 M H ₂ O/NaCl	1.7	100 ± 7	-	-	-
CPE-K ¹⁰	0.1 M H ₂ O/NaCl	~5	134	24.72 ± 6.9 /62.26 ± 6.2	300/2500	10/84
PEDOT-S: (Oct) ₂ NH ₂ ¹¹	1 M H ₂ O/KCl	-	-	8.3 ± 2.1	720	0.058
PEDOT-S: (Nonyl)NH ₃ ¹¹	1 M H ₂ O/KCl	-	-	6.4 ± 0.7	1110	0.062

Ethylene glycol (EG) is an additive utilized to improve electronic conductivity typically in PEDOT based and polythiophene based polymer. **CPE-K** is poly [2,6-(4,4-bis-potassium butylsulfonate-4H-cyclopenta-[2,1-b;3,4-b']dithiophene)-alt-4,7-(2,1,3-benzothiadiazole)]. **PEDOT-S** is poly(4-(2,3-dihydrothieno-(1,4)dioxin-2-yl-methoxy)-1-butanesulfonic acid), and **PEDOT-S: (Oct)₂NH₂** and **PEDOT-S: (Nonyl)NH₃** is PEDOT-S with a cation-exchanged dioctylammonium group, (Oct)₂NH₂, and nonylammonium group, (Nonyl)NH₃ group, respectively.

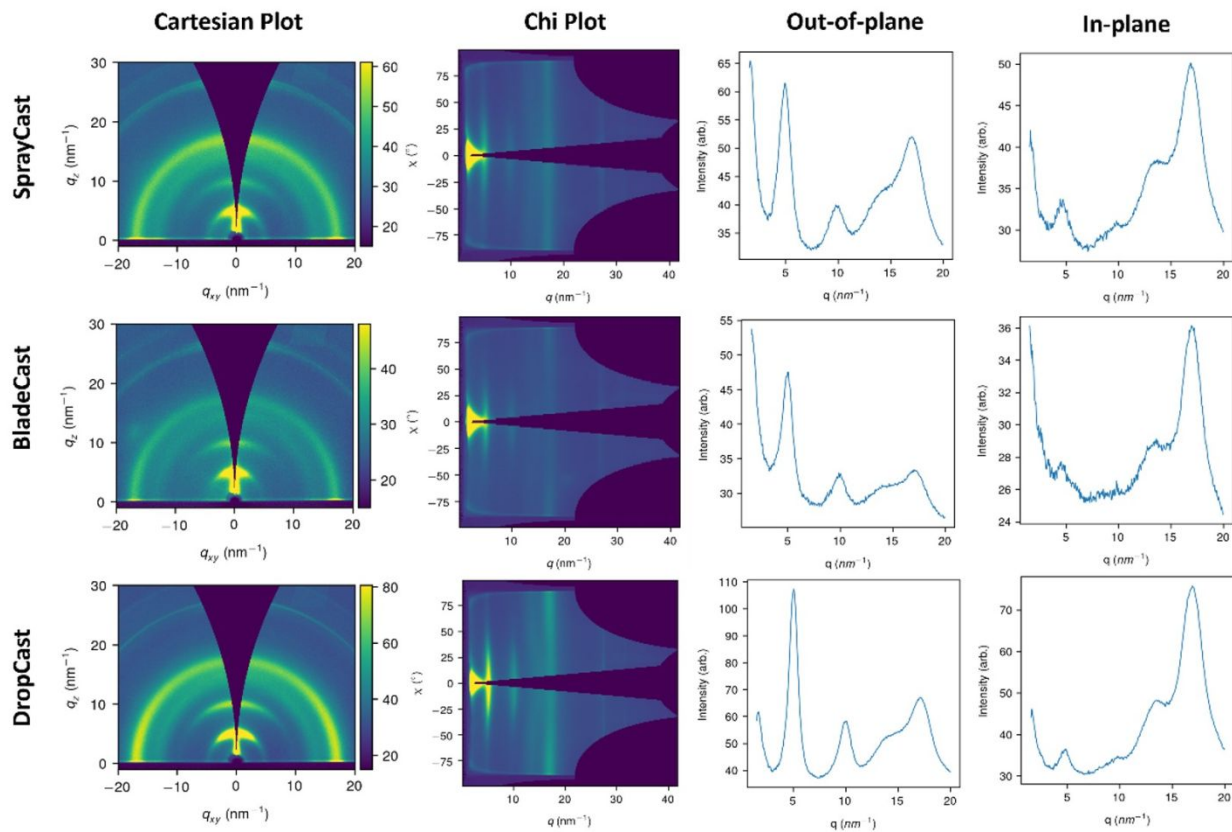


Figure S15: Cartesian and Chi-plots of the GIWAXS spectra for P3C(Pr)T in three cast techniques. These results demonstrate that processing potentially plays a minor role in dictating the as-cast microstructure of the polymer. P3C(Pr)T has a lamellar spacing (100) of 1.25 nm and a π -spacing (010) of 0.37 nm.

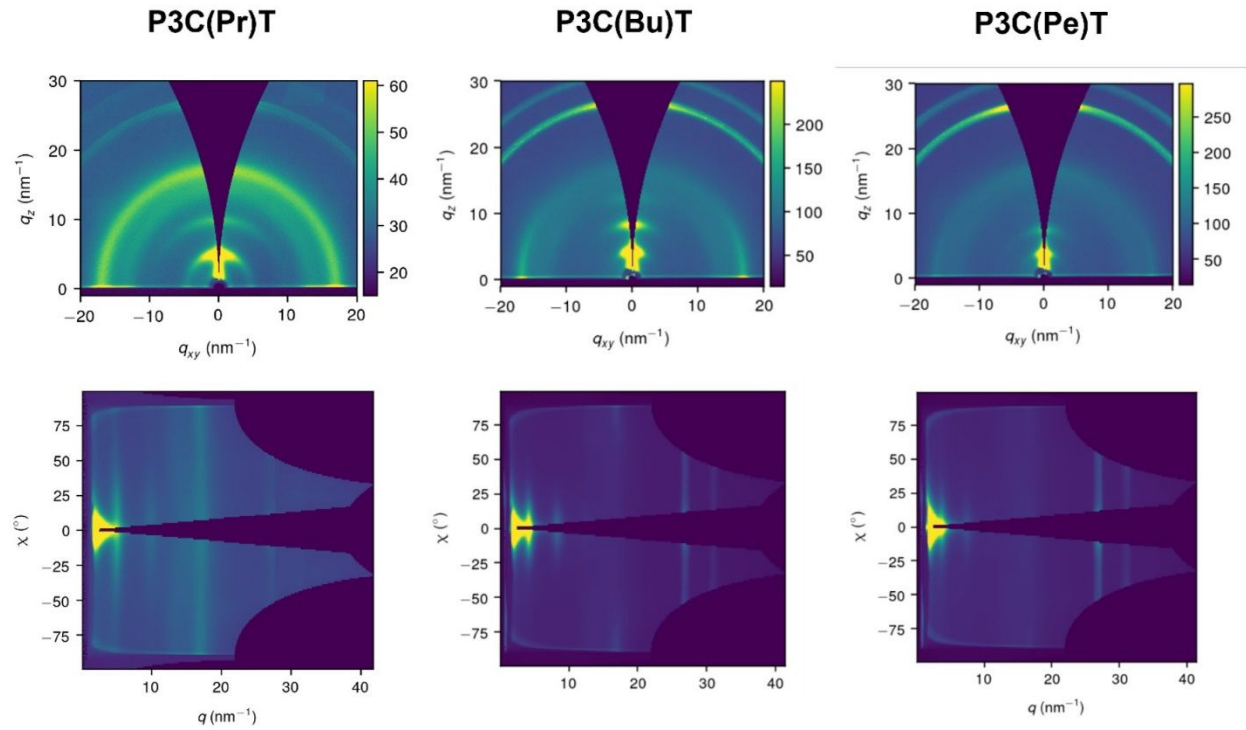


Figure S16: Cartesian and Chi-plots of the GIWAXS spectra for P3CAs though spray coating. P3C(Bu)T has a lamellar spacing (100) of 1.53 nm and P3C(Pe)T has a lamellar spacing (100) of 1.61 nm. Raw signal of π -spacing for Bu and Pe analogues is dim to perform further analysis. However, they appear to be around 0.372 nm, similar to P3C(Pr)T. These spectra provide clear evidence demonstrating the trend of expansion of the lamellar spacing as alkyl length increases.

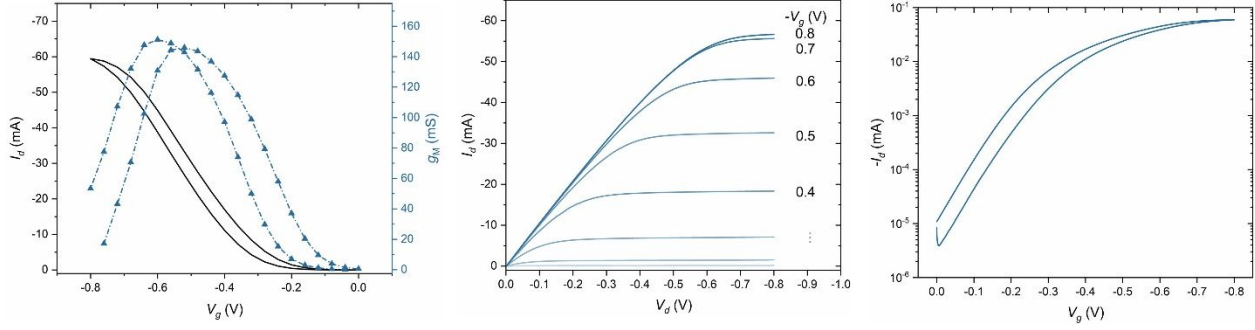


Figure S17: iOEET characteristics for P3C(Pr)T. From left to right, Transfer curve ($V_D = -0.6$ V) showing drain current varied with gate voltages (black line) and transconductance (dashed blue line). Output curve for various gate voltages; and transfer curve on logarithmic scale.

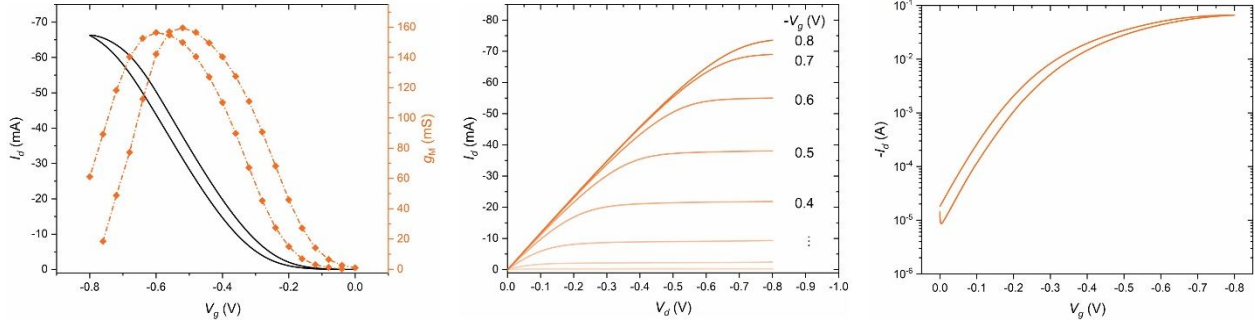


Figure S18: iOEET characteristics for P3C(Bu)T. From left to right, Transfer curve ($V_D = -0.6$ V) showing drain current varied with gate voltages (black line) and transconductance (dashed blue line). Output curve for various gate voltages; and transfer curve on logarithmic scale.

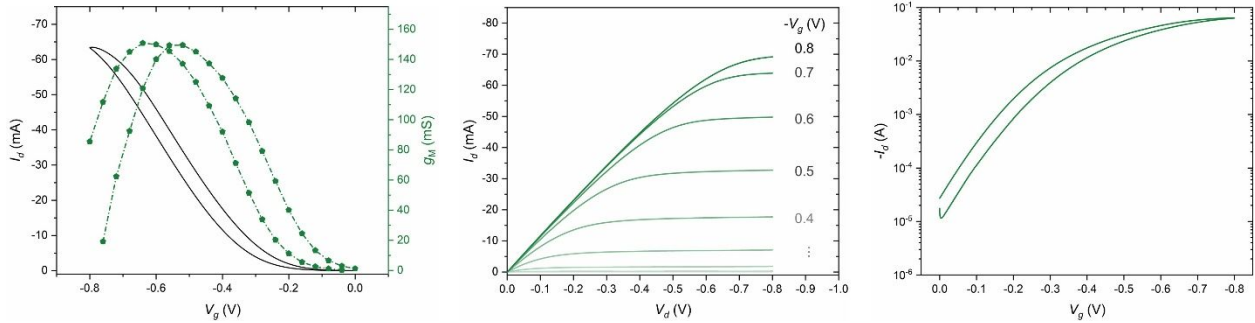


Figure S19: iOEET characteristics for P3C(Pe)T. From left to right, Transfer curve ($V_D = -0.6$ V) showing drain current varied with gate voltages (black line) and transconductance (dashed blue line). Output curve for various gate voltages; and transfer curve on logarithmic scale.

References

- (1) Nicolini, T.; Surgailis, J.; Savva, A.; Scaccabarozzi, A. D.; Nakar, R.; Thuau, D.; Wantz, G.; Richter, L. J.; Dautel, O.; Hadzioannou, G.; Stingelin, N. A Low-Swelling Polymeric Mixed Conductor Operating in Aqueous Electrolytes. *Advanced Materials* **2021**, *33* (2), 2005723. <https://doi.org/10.1002/adma.202005723>.
- (2) Savva, A.; Wustoni, S.; Inal, S. Ionic-to-Electronic Coupling Efficiency in PEDOT:PSS Films Operated in Aqueous Electrolytes. *J Mater Chem C Mater* **2018**, *6* (44), 12023–12030. <https://doi.org/10.1039/C8TC02195C>.
- (3) Savva, A.; Cendra, C.; Giugni, A.; Torre, B.; Surgailis, J.; Ohayon, D.; Giovannitti, A.; McCulloch, I.; Di Fabrizio, E.; Salleo, A.; Rivnay, J.; Inal, S. Influence of Water on the Performance of Organic Electrochemical Transistors. *Chemistry of Materials* **2019**, *31* (3), 927–937. <https://doi.org/10.1021/acs.chemmater.8b04335>.
- (4) Moser, M.; Wang, Y.; Hidalgo, T. C.; Liao, H.; Yu, Y.; Chen, J.; Duan, J.; Moruzzi, F.; Griggs, S.; Marks, A.; Gasparini, N.; Wadsworth, A.; Inal, S.; McCulloch, I.; Yue, W. Propylene and Butylene Glycol: New Alternatives to Ethylene Glycol in Conjugated Polymers for Bioelectronic Applications. *Mater Horiz* **2022**, *9* (3), 973–980. <https://doi.org/10.1039/D1MH01889B>.
- (5) Maria, I. P.; Paulsen, B. D.; Savva, A.; Ohayon, D.; Wu, R.; Hallani, R.; Basu, A.; Du, W.; Anthopoulos, T. D.; Inal, S.; Rivnay, J.; McCulloch, I.; Giovannitti, A. The Effect of Alkyl Spacers on the Mixed Ionic-Electronic Conduction Properties of N-Type Polymers. *Adv Funct Mater* **2021**, *31* (14), 2008718. <https://doi.org/10.1002/adfm.202008718>.
- (6) Schmode, P.; Ohayon, D.; Reichstein, P. M.; Savva, A.; Inal, S.; Thelakkat, M. High-Performance Organic Electrochemical Transistors Based on Conjugated Polyelectrolyte Copolymers. *Chemistry of Materials* **2019**, *31* (14), 5286–5295. <https://doi.org/10.1021/acs.chemmater.9b01722>.
- (7) Moser, M.; Hidalgo, T. C.; Surgailis, J.; Gladisch, J.; Ghosh, S.; Sheelamanthula, R.; Thiburce, Q.; Giovannitti, A.; Salleo, A.; Gasparini, N.; Wadsworth, A.; Zozoulenko, I.; Berggren, M.; Stavrinidou, E.; Inal, S.; McCulloch, I. Side Chain Redistribution as a Strategy to Boost Organic Electrochemical Transistor Performance and Stability. *Advanced Materials* **2020**, *32* (37), 2002748. <https://doi.org/10.1002/adma.202002748>.
- (8) Tsoi, W. C.; James, D. T.; Kim, J. S.; Nicholson, P. G.; Murphy, C. E.; Bradley, D. D. C.; Nelson, J.; Kim, J. S. The Nature of In-Plane Skeleton Raman Modes of P3HT and Their Correlation to the Degree of Molecular Order in P3HT:PCBM Blend Thin Films. *J Am Chem Soc* **2011**, *133* (25), 9834–9843. <https://doi.org/10.1021/JA2013104>.
- (9) Inal, S.; Malliaras, G. G.; Rivnay, J. Benchmarking Organic Mixed Conductors for Transistors. *Nat Commun* **2017**, *8* (1), 1767. <https://doi.org/10.1038/s41467-017-01812-w>.
- (10) Lill, A. T.; Cao, D. X.; Schrock, M.; Vollbrecht, J.; Huang, J.; Nguyen-Dang, T.; Brus, V. V.; Yurash, B.; Leifert, D.; Bazan, G. C.; Nguyen, T. Organic Electrochemical Transistors Based on the Conjugated

Polyelectrolyte PCPDTBT-SO₃ K (CPE-K). *Advanced Materials* **2020**, *32* (33), 1908120.
<https://doi.org/10.1002/adma.201908120>.

- (11) Zeglio, E.; Eriksson, J.; Gabrielsson, R.; Solin, N.; Inganäs, O. Highly Stable Conjugated Polyelectrolytes for Water-Based Hybrid Mode Electrochemical Transistors. *Advanced Materials* **2017**, *29* (19), 1605787. <https://doi.org/10.1002/adma.201605787>.